[Original paper]
Journal of the Korean Society for Nondestructive Testing
Vol. 31, No. 3 (2011. 6)

BWIM Using Measured Acceleration and Strain Data

Inyeol Paik*, Seon-Ung Lee** and Soobong Shin***†

Abstract A new BWIM(bridge weigh-in-motion) algorithm using both measured strain and acceleration data is proposed. To consider the effects of bridge vibration on the estimation of moving loads, the dynamic governing equation is applied with the known stiffness and mass properties but damping is ignored. Dynamic displacements are computed indirectly from the measured strains using the beam theory and accelerations are measured directly by accelerometers. To convert a unit moving load to its equivalent nodal force, a transformation matrix is determined. The incompleteness in the measured responses is considered in developing the algorithm. To examine the proposed BWIM algorithm, simulation studies, laboratory experiments and field tests were carried. In the simulation study, effects of measurement noise and estimation error in the vehicle speed on the results were investigated.

Keywords: BWIM, Strain and Acceleration, Vibration Effects, Transformation Matrix, Error Analysis

1. Introduction

Correct identification of loads moving over a bridge is essential for its maintenance and design[1]. Many experimental studies have been carried out on bridges to identify axle loads and to evaluate their live load effects on bridges [2-9]. Differently from WIM(weigh-in-motion) methods using sensors directly embedded on the road[6,10], a BWIM(bridge WIM) method estimates moving loads indirectly by using the measured bridge response[3]. Most available BWIM methods have been developed by using measured strains and static moment influence lines of a simply supported beam[11,12]. Because a bridge vibrates due to passing vehicles, however, the BWIM algorithms using the static moment influence lines cause inherent errors in estimating the moving loads. To overcome this problem, some dynamic algorithms have been developed and examined[13-19]. However, the available BWIM algorithms using dynamic responses could not be successfully applied to actual bridges because applications were limited to a single-degree- of-freedom system in some algorithms or because information on the state responses at all the degrees-of-freedom were required in the others.

The paper presents a BWIM algorithm using the structural dynamic governing equation. To apply it, structural matrices and state responses should be identified and provided. About the structural properties, stiffness and mass properties are assumed to be known but damping is ignored by assuming that its effects are negligible while loads are moving on a bridge. About structural responses, acceleration time histories can be usually measured by accelerometers in a field test. In addition, since damping is assumed to be negligible, velocity time histories need not be obtained in the proposed algorithm. However, displacement time

[Received: April 12, 2011, Revised: May 30, 2011, Accepted: June 3, 2011] *Dept. of Civil & Environmental Eng., Kyungwon University, Songnam-si 461-701, Korea, **ESCO C&S, Anyang-si 431-060, Korea, ***Dept. of Civil Eng., Inha University, Incheon 402-751, Korea, †Corresponding Author: sbshin@inha.ac.kr

histories should be measured or determined by any means. When displacement time history is computed numerically by integrating measured acceleration, numeric errors in its calculation cannot be avoided. Some methods for directly measuring or computing displacement time history have been introduced but the results may not so reliable yet[20]. In the proposed algorithm, displacement time history is analytically computed from measured strain data by using the beam theory. Also, since it is difficult to measure responses at all the degrees of freedom, responses at the unmeasured degrees of freedom are numerically computed by the mode superposition.

The equivalent force vector in the dynamic governing equation is converted from a unit moving load by using a transformation matrix. Since vehicles pass over a bridge in various speeds and the resulting equivalent nodal forces also vary depending on the speed, a nodal force transformation matrix was constructed at each vehicle speed and applied to estimate moving loads inversely. However, since the shapes of transformation matrices are equal regardless of the vehicle speed, a standard form is determined and then shortened or elongated with time for a different vehicle speed.

To examine the proposed BWIM algorithm, simulation studies, laboratory and also field tests were carried out. In the simulation study, the effects of error in vehicle speed and measurement noise on the estimation results were investigated. The speed error can be considered as the same as the position error of a vehicle in time.

2. BWIM Algorithm Considering Dynamic Effects

2.1 Dynamic Governing Equation

The structural dynamic governing equation is defined by eqn. (1).

$$\mathbf{M}\ddot{u}(t)+\mathbf{C}\dot{u}(t)+\mathbf{K}\mathbf{u}(t)=\mathbf{f}(t) \quad (1)$$

where $\mathbf{M}(N\times N)$, $\mathbf{C}(N\times N)$, $\mathbf{K}(N\times N)$ = mass, damping, and stiffness, $\ddot{\mathbf{u}},\dot{\mathbf{u}},\mathbf{u},\mathbf{f}$ = acceleration, velocity, displacement, and force vector at time t, and N = number of degrees of freedom (DOF), respectively.

In applying eqn. (1), it has been assumed that mass and stiffness properties can be determined from the given material and sectional information or also can be identified through an application of a system identification[21]. It has been also assumed that damping force can be ignored by assuming that the transient part of vibration can be ignored while loads are moving on a bridge. With these assumptions, eqn. (1) can be reduced to eqn. (2). Therefore, it is required to measure or formulate acceleration $\ddot{\mathbf{u}}$ and displacement $\mathbf{u}$ vectors at each time step to identify force vector $\mathbf{f}$ directly from eqn. (2).

$$\mathbf{M}\ddot{u}(t)+\mathbf{K}\mathbf{u}(t)=\mathbf{f}(t) \quad (2)$$

2.2 Computation of Unmeasured Responses

Actual civil structures usually include many DOFs in finite element modeling. However, some DOFs are hard to be measured directly even with current advanced technologies. Usual field measurements include acceleration and strain time history data to the limited DOFs of a structure. Therefore, it is highly required to develop an algorithm which can take account of the incompleteness in both space and state of measured data.

2.2.1 Computation of Unmeasured Acceleration

To consider the incompleteness in space when accelerations are measured at limited DOFs, acceleration can be divided into measured and unmeasured parts at each time step and can be related to the modal information as eqn. (3).

$$\ddot{\mathbf{u}}(t)=\begin{Bmatrix}\ddot{\mathbf{u}}_m(t)\\ \ddot{\mathbf{u}}_u(t)\end{Bmatrix}=\begin{bmatrix}\Phi_m\\ \Phi_u\end{bmatrix}\ddot{\mathbf{q}}(t)=\Phi\,\ddot{\mathbf{q}}(t) \tag{3}$$

where $\ddot{\mathbf{u}}_m(N_m\times 1), \ddot{\mathbf{u}}_u(N_u\times 1)$ = measured and unmeasured part of acceleration vector at time step t, $\Phi_m(N_m\times N_{md}), \Phi_u(N_u\times N_{md})$ = measured and unmeasured part of mode shape matrix $\Phi(N\times N_{md})$, $\ddot{\mathbf{q}}(N_{md}\times 1)$ = double differentiation of generalized coordinate vector with respect to time t, N_m, N_u = number of measured and unmeasured DOFs, and N_{md} = number of utilized modes, respectively. The separation of eqn. (3) can be identically applied to the displacement vector as well.

Since the system matrices of **M** and **K** were assumed as known information, the mode shape matrix Φ can be computed numerically. Therefore, by the least squared approach, acceleration response at unmeasured DOFs can be obtained by eqn. (4).

$$\begin{aligned}\ddot{\mathbf{q}}&=\left[\Phi_m^T\quad\Phi_m\right]^{-1}\Phi_m^T\,\ddot{\mathbf{u}}_m\\ \ddot{\mathbf{u}}_u&=\Phi_u\,\ddot{\mathbf{q}}\end{aligned} \tag{4}$$

Since eqn. (4) is basically least-squared, the identifiability criterion of eqn. (5) should be satisfied to prevent an under-determined system of equations where multiple solutions may be obtained. The identification results may be usually improved when more modes are involved in the computation. In the current approach, therefore, the number of required modes from the numerical computation is fixed as equal to the number of measured DOFs.

$$N_{md}\le N_m \tag{5}$$

2.2.2 Computation of Displacement

Any reliable scheme has not been developed to measure dynamic displacements directly from a structure. A double integration of acceleration with initial conditions usually cannot result in reliable displacement time history. Jeong et al.[20] proposed a method using wavelet decomposition signal of measured acceleration and applied it to actual bridge responses. But the results are highly dependent on the selection of some important time steps required to apply the algorithm. Only a skilled engineer seems to select them properly.

In the current context of the algorithm, displacements are to be computed from dynamic strain measured at the same locations as the accelerometers. Since the bending behavior is dominant in the girders of a bridge in the longitudinal direction, the following relationship of eqn. (6) can be formulated from the beam theory.

$$\boldsymbol{\varepsilon}_m(x,t)=-y_c\,\mathbf{u}_m''(x,t)=-y_c\,\Phi_m''(x)\,\mathbf{q}(t) \tag{6}$$

where $\mathbf{u}_m''(N_m\times 1)$, $\Phi_m''(N_m\times N_{md})$ = double differentiation of displacement vector and mode shape matrix with respect to the coordinate x in the longitudinal direction, $\boldsymbol{\varepsilon}_m(N_m\times 1)$ = strain measured at the same locations of accelerometers, $\mathbf{q}(N_{md}\times 1)$ = generalized coordinate related to the strain, yc = distance from the neutral axis, respectively. Since the beam theory is applied in the formulation, theoretical values of Φ_m'' can be easily computed at the locations of strain gage.

The generalized coordinate **q** can be computed at each time step t by eqn. (7) and then the whole displacement vector can be computed by eqn. (8).

$$\mathbf{q}=\left[\Phi_m''^T\quad\Phi_m''\right]^{-1}\Phi_m''^T\,\boldsymbol{\varepsilon}_m \tag{7}$$

$$\mathbf{u}=\Phi\,\mathbf{q} \tag{8}$$

2.3 Transformation of Moving Loads to Equivalent Nodal Force

The force vector **f** in eqn. (2) is an

equivalent nodal force in a discretized finite element model. Since actual loads are moving on a bridge, however, it is required to relate moving loads to the equivalent nodal force as eqn. (9). The actual loads can be obtained by the least squared formulation of eqn. (10).

$$\mathbf{f}(t) = \mathbf{T}(t, v)\,\mathbf{p}(t) \tag{9}$$

$$\mathbf{p}(t) = \left[\mathbf{T}(t)^T\,\mathbf{T}(t)\right]^{-1}\mathbf{T}(t)^T\,\mathbf{f}(t) \tag{10}$$

where $\mathbf{T}(N\times N_p)$ = transformation matrix between the equivalent nodal force $\mathbf{f}(N\times 1)$ and actual loads $\mathbf{p}(N_p\times 1)$ in a constant vehicle velocity v and N_p = the number of axle loads passing over a bridge.

In numerical analysis, exact nodal force is applied as a triangular shape as shown in Fig. 1. When dynamic response is simulated through modal superposition with the consideration on the unmeasured DOFs, however, nodal force changes to the shape of an oscillating one in Fig. 1. The shape varies depending on the number of measured DOFs but can be fixed after the measurement layout is determined. The qualitative shape of the nodal force does not change so that it can be shortened or elongated in time depending on the vehicle speed. Therefore, for simplicity, a database can be constructed for various vehicle speeds with a consistent time increment.

3. Examination of the Algorithm by Simulation Studies

3.1 Application to a Simply Supported Beam

For the simulation study, a simple beam of Fig. 2 has been utilized. The analytical solution for the beam under a moving unit load given in Biggs[22] was applied as in eqn. (11). The vibration responses of the beam were simulated by the superposition of a hundred modes.

$$u(x,t) = \frac{2p}{mL}\sum_{r=1}^{N_{max}} \frac{\sin\Omega_r t - \Omega_r/\omega_r \sin\omega_r t}{\omega_r^2 - \Omega_r^2}\sin\frac{r\pi x}{L} \tag{11}$$

where $\Omega_r = r\pi v/L$ and ω_r = natural rotational frequency of the beam.

A transformation matrix was constructed as Fig. 3 with a constant sampling rate. In the figure, a curve of dotted line is the computed nodal forces with the moving unit load at each measuring point. The values at the sampling points of circles in each solid line are the values for the transformation matrix. Tale of each dotted line with negative values in most part was truncated.

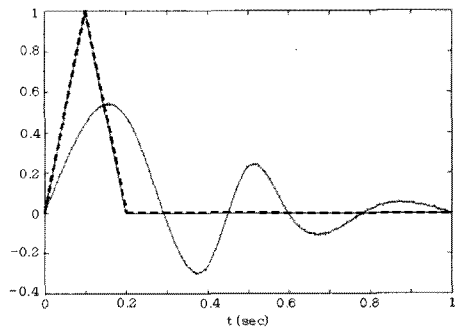

Fig. 1 Comparison of unit load and its nodal force

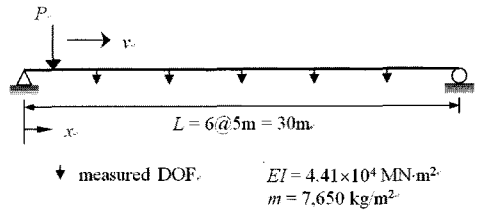

Fig. 2 Simple beam for the simulation study

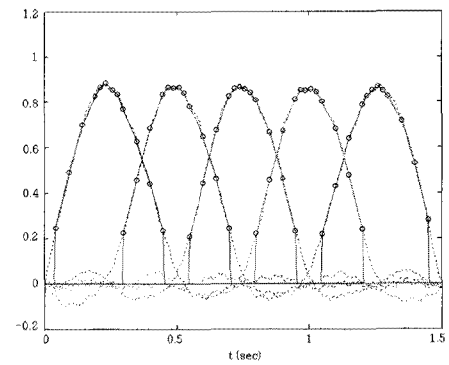

Fig. 3 Construction of a transformation matrix

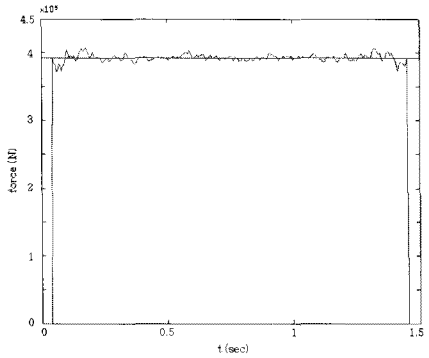

Fig. 4 Identified moving load using truncated transformation data

Fig. 4 shows the identified moving load when a single load of 390kN passed over the beam and measurement noise was not considered in the simulation. The averaged identification error was as small as 0.4%. The proposed algorithm could provide perfect matches theoretically if noise-free responses are applied and all the nodal force data are used without truncation.

3.2 Effects of Velocity Error

The proposed algorithm has assumed that each load moves in a constant velocity on the bridge and the moving speed can be detected. In actual applications, however, it may not be easy to check the actual moving speed of a vehicle correctly. Also, a vehicle speed can vary during its running on a bridge. Therefore, the effects of velocity error should be investigated.

For the simulation study, proportional errors in the vehicle speed were simulated and the results are compared in Fig. 5. From these figures, it can be observed that the identification results oscillate more severely around when the load moved out of the beam as velocity error increased. The averaged identification errors are summarized in Table 1 with respect to the velocity error. The results illustrate the importance of correct determination of vehicle speed for reliable force identifications.

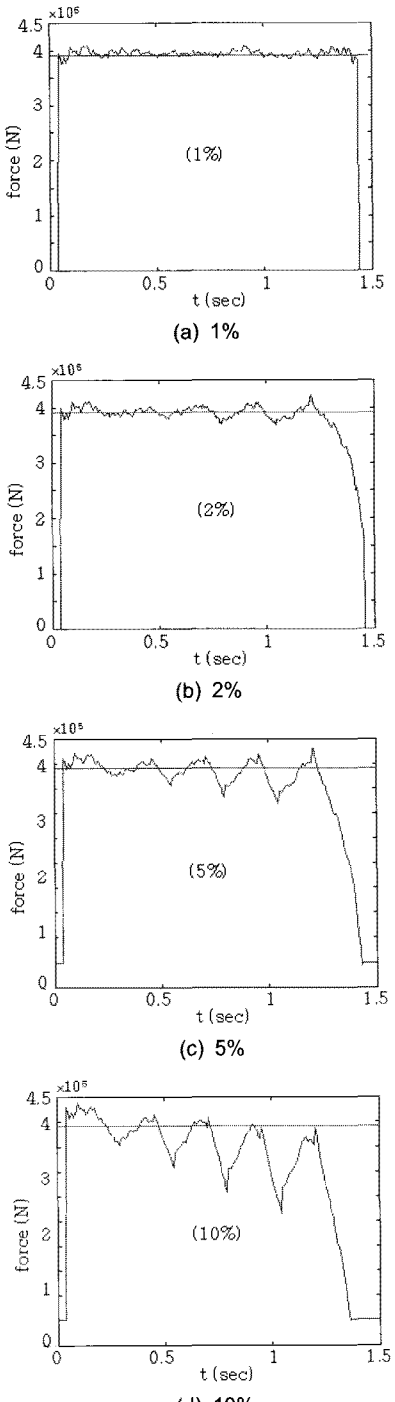

Fig. 5 Identified moving loads with the velocity errors

Table 1 Identification error with the velocity error

Velocity error	1%	2%	5%	10%
Identification error (%)	0.944	0.408	3.49	13.00

3.3 Effects of Measurement Noise

Noise is indispensable from field measurements in nature. In the current simulation study, absolute white noise was implemented in random. Since the proposed algorithm of eqn. (2) requires computing accelerations at unmeasured DOFs and displacements at all the DOFs, effects of noise in acceleration and strain data on the identification results were investigated separately.

Fig. 6 compares the identified results of a single moving load when 1% proportional noise was simulated in acceleration and in strain data, respectively. The algorithm requires acceleration and displacement responses as expressed in eqn. (2) and displacements were computed from strain data from eqn. (7) and eqn. (8). From Fig. 6, it can be observed that noise in strain data deteriorates the accuracy of the identified results more severely. However, even with noise

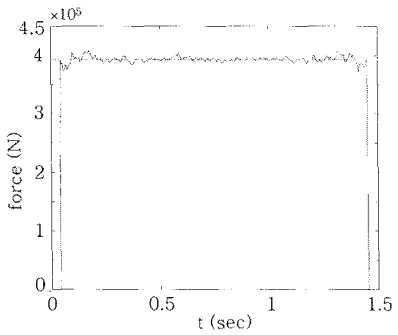

(a) Noise in acceleration

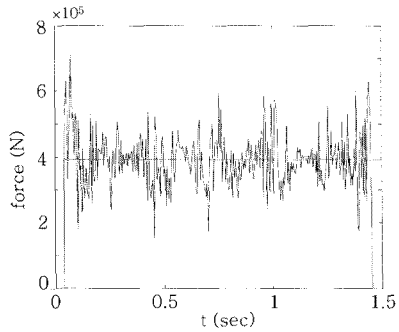

(b) Noise in strain

Fig. 6 Identified moving loads with different type of noise

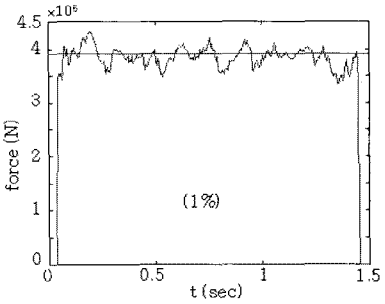

(a) 1%

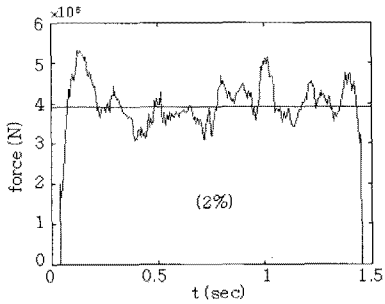

(b) 2%

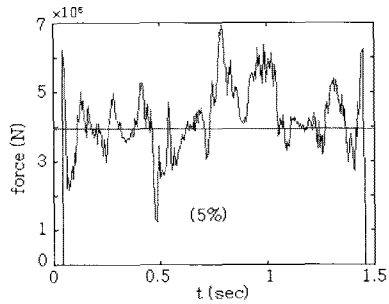

(c) 5%

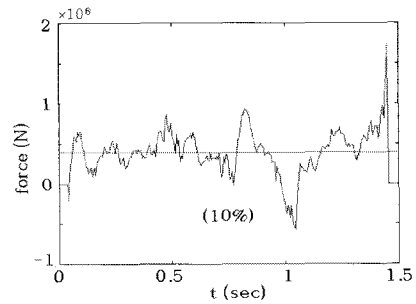

(d) 10%

Fig. 7 Identified moving average with different type of noise

Table 2 Identification error with the measurement noise

Velocity error	1%	2%	5%	10%
Identification error (%)	1.33	0.92	9.01	5.26

in strain data, the overall trend of the identified results oscillates around the actual value in a quite symmetric manner. Therefore, the moving average scheme was applied to average out the severe identification error. However, if we can develop and apply a method to measure deflections directly, then the noise due to strain measurements may be reduced.

Fig. 7 shows the identified results obtained by the moving average of the estimated values with proportional errors in both acceleration and strain data. The identification errors are compared in Table 2. Even if the trend is not so consistent as shown in Table 2, the averaged identification error increases as the noise level is increased in general.

4. Validation of the Algorithm through Laboratory Experiments

To validate the applicability of the proposed algorithm, laboratory experiments were carried out. The model steel bridge of 6m long and the model vehicle are shown in Fig. 8. The sectional dimensions of the model bridge and vehicle types of test cases are drawn in Fig. 9. The model vehicles were controlled to move in a constant speed on the bridge. The distance between two axles of a model truck was 28.5 cm which is less than 1/20 of the length of the bridge and is too short to identify the weight of both axles reasonably.

Five accelerations were measured to the vertical direction at an equal distance on both sides of the bridge so that all the ten vertical acceleration time histories were measured during the vibration. Longitudinal strains were also measured at the same locations as the accelerometers below the side flanges. Since noise in strain data is more critical for reliable identification as demonstrated from the simulation study, strains were measured by fiber optic sensors rather than usual electric-type strain gages.

Before carrying out the moving load tests, mass and stiffness properties of the beam model were identified using measured modal data obtained from impact hammer tests. The model was also verified through static load tests by comparing measured and computed vertical displacements at different locations.

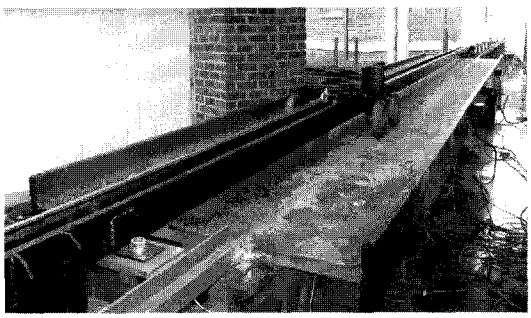

Fig. 8 Model bridge and vehicle for laboratory tests

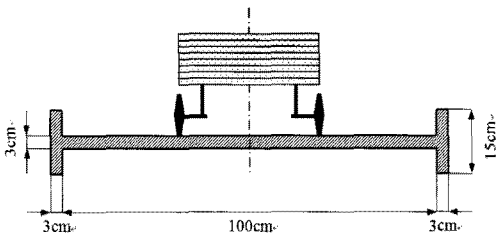

(a) Sectional dimensions

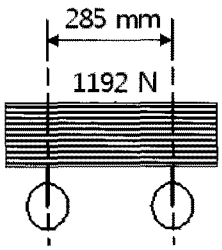

(b) One-vehicle case

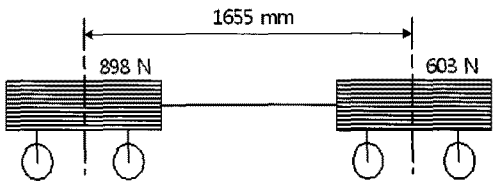

(c) Two-vehicle case

Fig. 9 Sectional dimensions and vehicle type for each test case

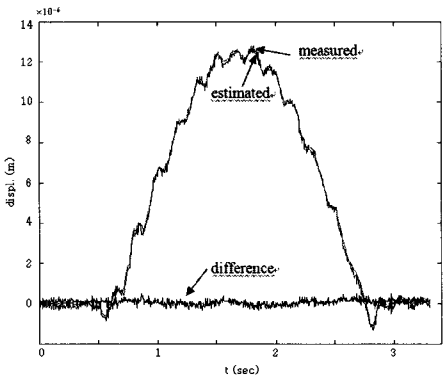

Fig. 10 Comparison of displacements measured from LVDT and those from strains

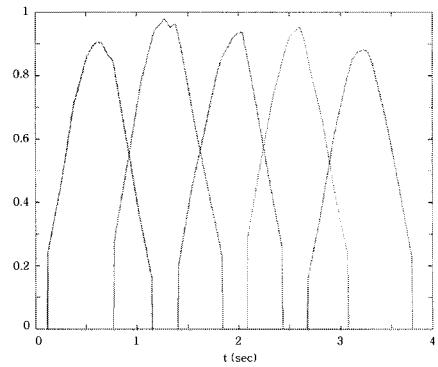

Fig. 11 Transformed nodal force

Fig. 10 compares the displacements measured from LVDT and those obtained from measured strain data by eqn. (8). The closeness of the two displacement results demonstrates the usefulness of the strain measurements, even though negligibly small fluctuation of displacements computed from strain data could be observed. The oscillating signal at the bottom of the figure indicates the difference between the two curves. Fig. 11 shows the nodal force data for the transformation matrix.

4.1 Case I: One Vehicle

As the first trial case, one model vehicle of Fig. 9(b) moved on the bridge with various speeds. Dynamic responses of accelerations and strains were measured and the vehicle load was identified as a single load along the beam.

The identified results are drawn in Fig. 12 for the speed of 1.54 m/sec and 2.85 m/sec, respectively. Regardless of the vehicle speeds, the trends of the two cases are almost identical. In both speeds, the identified forces gradually decrease as the vehicle approaches to the end of the bridge. The averaged identification errors are summarized in Table 3.

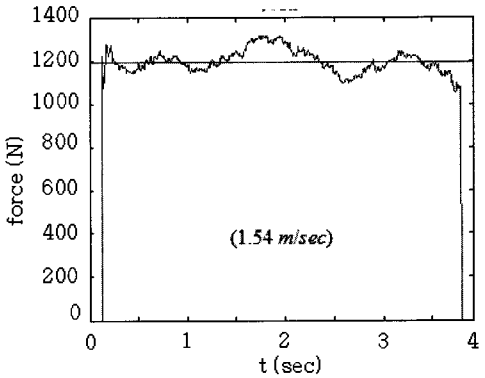

(a) 1.54m/sec

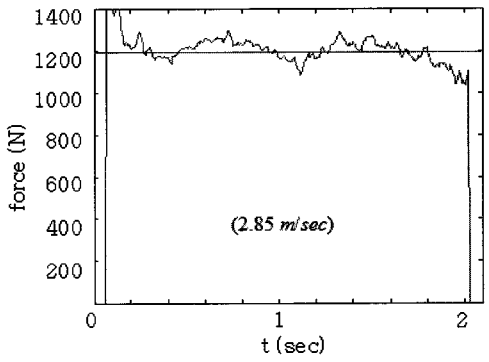

(b) 2.85m/sec

Fig. 12 Identified moving vehicle in two different speeds

Table 3 Identification errors in different vehicle speeds

Case	Velocity (m/sec)		Identification error (%)
I (one vehicle)	1.54		0.92
	2.85		1.26
II (two vehicles)	1.11	vehicle 1	3.15
		vehicle 2	2.00
	1.91	vehicle 1	0.33
		vehicle 2	0.89

4.2 Case II: Two Vehicles

Two model vehicles were linked together by a buckle as shown in Fig. 9(c) so that two vehicles moved in the same constant speed over the bridge. Since the axle distance of each truck is too small, two vehicles were identified as two concentrated loads.

The identified results are drawn in Fig. 13 for the speed of 1.11 m/sec and 1.91 m/sec, respectively. From the figure, it can be observed that the identification of the front load sharply jumped when the front vehicle moved out of the bridge while that of the rear load sharply jumped when the rear vehicle entered the bridge. Both numerical jumps occurred when the number of estimated loads was suddenly changed. The identification errors are also summarized in Table 3 and the results demonstrate that the vehicle loads could be reliably identified within a tolerable error even with those sharp jumps.

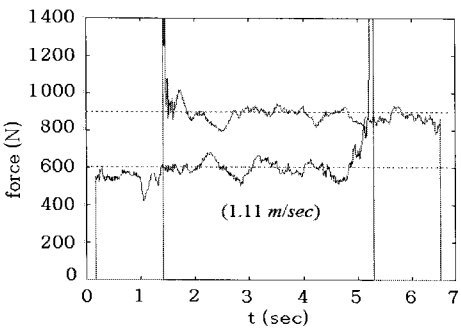

(a) 1.11m/sec

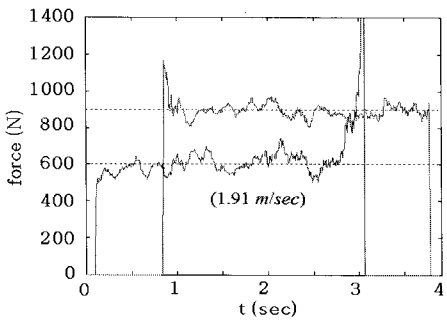

(a) 1.91m/sec

Fig. 13 Identified forces of two moving trucks in two different speeds

5. Application of the Algorithm to a Field Test

The proposed algorithm was applied to a field test on a simply supported plate-girder bridge of 39.8 m span length locating in an express highway in Korea as shown in Fig. 14. As shown in the figure, fifteen accelerometers and FBG sensors were installed under the bridge so that three of each type of sensor was located in the half of each girder. Five LVDTs were installed in the middle of each girder to validate the computed displacements from measured strains. Piezo sensors were placed in front of the

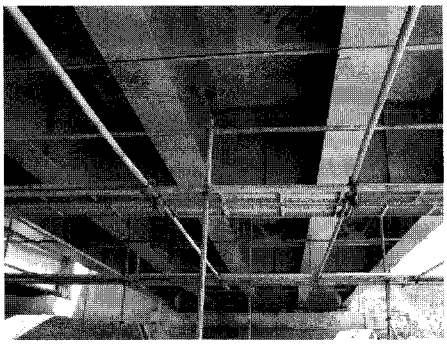

(a) Plate-girder bridge

(b) Truck for the test

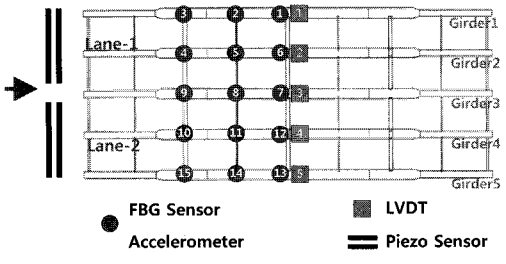

(c) Sensor layout

Fig. 14 Plate-girder bridge and the test layout

bridge to check the location of a moving truck. Because the total truck load was determined by summing the partially identified load from each girder, load distribution on each girder was not considered. In other words, equal load distribution on each girder was simply assumed.

Some test cases were carried out but only the responses from the case with a single truck moving on the bridge could be reliably used, because some FBG sensors were malfunctioned due to manufacturing problems. Also, the number of sensors for each girder was limited to three even the total number of accelerometers was fifteen. As a result, the computed displacements in Fig. 15 show relatively large gaps from those measured by LVDTs even for the case of a single truck. To improve the accuracy, the number of each type of sensors should have been increased more than five on each girder as tested through simulation studies and laboratory experiments. Also, the maximum displacements in each girder were quite small values of less than 3 mm.

Since all the data were measured only in the half of the bridge span and the ratio of the truck axle distance to the half span length is

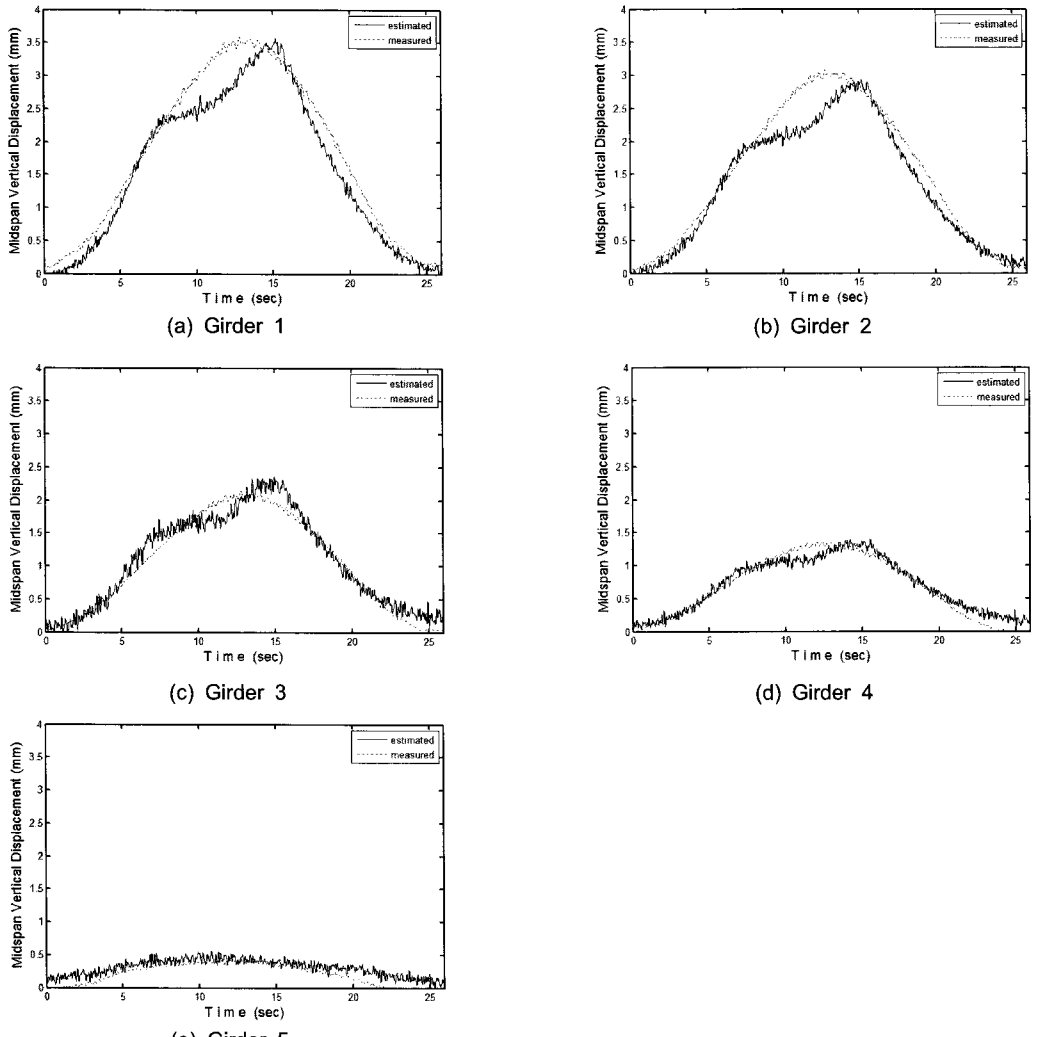

(a) Girder 1 (b) Girder 2

(c) Girder 3 (d) Girder 4

(e) Girder 5

Fig. 15 Comparison of computed displacements with those measured by LVDTs

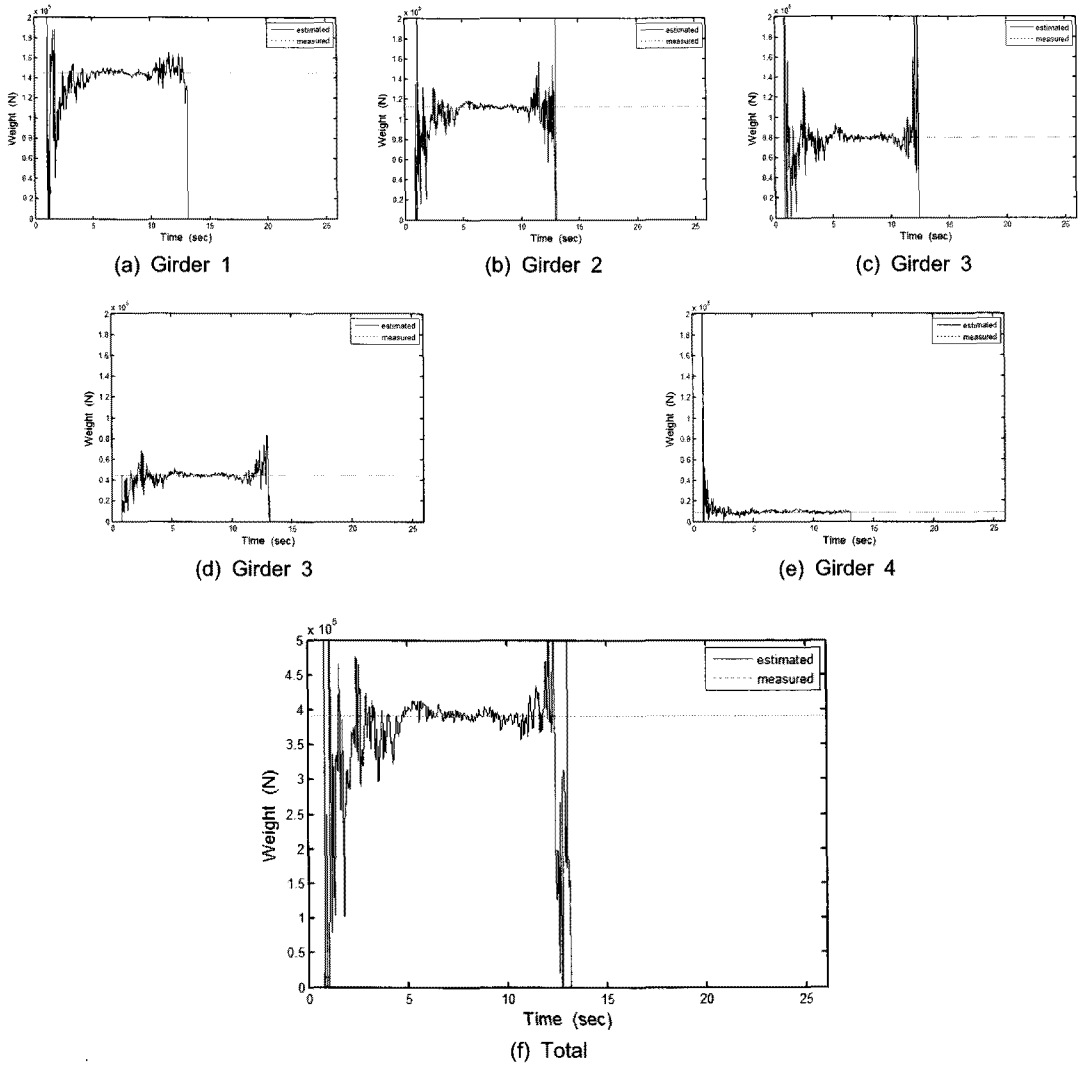

Fig. 16 Identified truck load

4.725 m/19.9 m = 0.24, each axle load could not be correctly identified. However, the total truck load could be identified correctly as shown in Fig. 16. The truck load was obtained by summing up the identified load from each girder as shown in Fig. 16. The identified total load was 390.518 kN with 2% error from actual truck load of 391.187 kN.

6. Conclusions

A BWIM algorithm considering bridge vibration is proposed by measuring acceleration and strain time histories simultaneously. Dynamic displacements were computed from the measured strains by the beam theory. In the algorithm, responses at the unmeasured DOFs were computed numerically by the mode superposition. A force transformation matrix was defined to relay an actual moving load to an equivalent nodal force at each DOF. In the dynamic governing equation, mass and stiffness properties were assumed to be known a priori but damping was ignored.

The algorithm has been examined successfully through simulation studies and

laboratory experiments. It has been also applied to field tests but the field applications could not demonstrate its efficiency properly due to the malfunctioned FBG sensors and the improperness in the sensor layout. However, the identified results from the overall study could illustrate the usefulness of the proposed idea.

In the simulation study, the effect of the error in the vehicle speed and that of the measurement noise on the identified results were investigated. The error in the estimated vehicle speed accelerated as the vehicle approached to the end-gate of the bridge. Within less than 5% error in the vehicle speed, the identification error was relatively small. About the measurement noise, noise in acceleration and strain data were separately investigated. Through the simulation study, it could be observed that noise in strain data could influence on the identified results more severely than that in acceleration. However, by using the moving average scheme, the identified results could be improved.

Acknowledgement

This study was supported by KICTEP under the Grant 08-E01 of Super Long Span Bridge Project and Inha University.

References

[1] A. S. Nowak and K. R. Collins, "*Reliability of Structures*," McGraw-Hill, Inc. (2000)

[2] A. T. Dempsey, B. Jacob and J. Carracilli, "Orthotropic bridge weigh-in-motion for determining axle and gross vehicles weights," *Proceedings of the Second European Conference on WIM,* pp. 345-354 (1998)

[3] D. Dunne, E. J. O'Brien, B. Basu and A. Gonzalez, "Bridge WIM systems with nothing on the road(NOR)," *Proceedings of ICWIM4,* Taipei Taiwan, February, pp. 119-127 (2005)

[4] M. Ghosun and B. Sivakumar, "Using weigh-in-motion data for modeling maximum live load effects on highway bridges," IABMAS2010, *Proceedings of Bridge Maintenance, Safety, Management and Life-Cycle Optimization,* pp. 939-945 (2010)

[5] M. Kozikowski and A. S. Nowak, "Live load models based on weigh-in-motion data," IABMAS2010, *Proceedings of Bridge Maintenance, Safety, Management and Life-Cycle Optimization,* pp. 2881-2888 (2010)

[6] A. S. Nowak, S. Kim and V. Saraf, "Monitoring truck loads and field testing of bridges," *Proceedings of the International Seminar on New Technologies for Bridge Management,* Seoul Korea, December, pp. 219-248 (1996)

[7] E. J. O'brien, A. Hayrapetova and C. Walsh, "Micro-simulation modeling of traffic loading on medium- and long-span road bridges," IABMAS2008, *Proceedings of Bridge Maintenance, Safety, Management, Health Monitoring and Informatics,* pp. 2353-2359 (2008)

[8] T. Ueda, K. Taniguchi and H. Sato, "Estimation of multiple-sensor weigh-in-motion, *Proceedings of ICWIM4,* Taipei Taiwan, February, pp. 27-33 (2005)

[9] A. Znidaric, I. Lavric and J. Kalin, "Latest practical developments in the bridge WIM technology," IABMAS2010, *Proceedings of Bridge Maintenance, Safety, Management and Life-Cycle Optimization,* pp. 994-1000 (2010)

[10] T. Ojio and K. Yamada, "Bridge WIM by reaction force method," *Proceedings of ICWIM4,* Taipei Taiwan, February, pp. 107-118 (2005)

[11] B. Jacob and E. J. O'Brien, "Weigh-in-motion: recent developments in Europe," *Proceedings of ICWIM4,* Taipei Taiwan, February, pp. 3-13 (2005)

[12] C. O'Connor and T. H. T. Chan, "Dynamic loads from bridge strains," *Journal of Structural Engineering,* ASCE, Vol. 114, pp. 1703-1723 (1988)

[13] T. H. T. Chan, S. S. Law, T. H. Yung and X. R. Yuan, "An interpretive method for moving force identification," *Journal of Sound and Vibration*, Vol. 219, No. 3, pp. 503-529 (1999)

[14] R. J. Jiang, F. T. K. Au and Y. K. Cheung, "Identification of masses moving on multi-span beams based on a genetic algorithm," *Computers and Structures,* Vol. 81, pp. 2137-2148 (2003)

[15] S. S. Law, T. H. T. Chan and Q. H. Zeng, "Moving force identification: a time domain method," *Journal of Sound and Vibration*, Vol. 201, pp. 1-22 (1997)

[16] S. S. Law, T. H. T. Chan and Q. H. Zeng, "Moving force identification-a frequency and time domain analysis," *Journal of Dynamic System, Measurement and Control,* Vol. 121, pp. 394-401 (1999)

[17] L. Yu, "Moving force identification based on the frequency-time domain method," *Journal of Sound and Vibration*, Vol. 261, No. 1, pp. 329-349 (2002)

[18] X. Q. Zhu and S. S. Law, "Dynamic axle and wheel loads identification: laboratory studies," *Journal of Sound and Vibration*, Vol. 268, pp. 855-879 (2003)

[19] X. Q. Zhu and S. S. Law, "Identification of moving interaction forces with incomplete velocity information," *Mechanical Systems and Signal Processing,* Vol. 17, No. 6, pp. 1349-1366 (2003)

[20] B. S. Jeong, N. S. Kim and S. K. Kook, "Estimation of displacement responses using the wavelet decomposition signal," *Journal of the Korea Concrete Institute*, Vol. 18, No. 3, pp. 347-354 (2006)

[21] S. Shin and H. Oh, "Damage assessment of shear buildings by synchronous estimation of stiffness and damping using measured acceleration," *Smart Structures and Systems,* Vol. 3, No. 3, July, pp. 245-261 (2007)

[22] J. M. Biggs, "Introduction to Structural Dynamics,"McGraw-Hill, Inc. (1982)